

# Structural Relaxation and Viscoelasticity of a Higher Alcohol with Mesoscopic Structure

*Tsuyoshi Yamaguchi,<sup>1,\*</sup> Makina Saito,<sup>2</sup> Koji Yoshida,<sup>3</sup> Toshio Yamaguchi,<sup>3</sup> Yoshitaka Yoda,<sup>4</sup> and Makoto Seto<sup>2</sup>*

<sup>1</sup> Graduate School of Engineering, Nagoya University, Furo-cho B2-3 (611), Chikusa, Nagoya, Aichi 464-8603, Japan.

<sup>2</sup> Research Reactor Institute, Kyoto University, Kumatori, Osaka 590-0494, Japan.

<sup>3</sup> Department of Chemistry, Faculty of Science, Fukuoka University, Nanakuma, Jonan, Fukuoka 814-0180, Japan.

<sup>4</sup> Research and Utilization Division, Japan Synchrotron Radiation Research Institute, Kouto, Sayo-cho, Sayo-gun, Hyogo 679-5198, Japan.

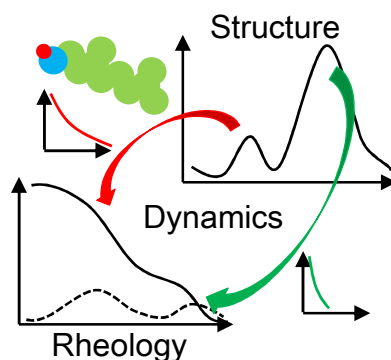
## AUTHOR INFORMATION

### Corresponding Author

\* E-mail to Tsuyoshi Yamaguchi: [yamaguchi.tsuyoshi@material.nagoya-u.ac.jp](mailto:yamaguchi.tsuyoshi@material.nagoya-u.ac.jp)

1  
2  
3 This work studied the slow dynamics of liquids with mesoscopic structure and its relation to  
4 shear viscosity. Quasielastic scattering measurements were made on a liquid higher alcohol, 3,7-  
5 dimethyl-1-octanol, using  $\gamma$ -ray time-domain interferometry at a synchrotron radiation facility,  
6  
7  
8 dimethyl-1-octanol, using  $\gamma$ -ray time-domain interferometry at a synchrotron radiation facility,  
9  
10 SPring-8. The quasielastic scattering spectra were measured to determine the structural  
11 relaxation at two wavenumbers of the prepeak and the main peak of the static structure factor. It  
12  
13 relaxation at two wavenumbers of the prepeak and the main peak of the static structure factor. It  
14  
15 was found that relaxation at the prepeak is more than 10 times slower than that at the main peak.  
16  
17 Compared with the viscoelastic spectrum, which exhibits bimodal relaxation, the relaxations at  
18  
19 the prepeak and the main peak were shown to correspond to the slower and faster modes of the  
20  
21 viscoelastic relaxation, respectively. This indicates that the dynamics of the mesoscopic  
22  
23 structure represented as the prepeak contributes to the shear viscosity through the slowest mode  
24  
25 of the viscoelastic relaxation.  
26  
27  
28  
29

## 30 TOC GRAPHICS



1  
2  
3 The properties of liquids with mesoscopic structures have attracted many researchers for a  
4 decade. The intermolecular correlation in simple liquids appears at a wavenumber  
5  
6 corresponding to the contact distance, usually  $10 \text{ nm}^{-1} - 20 \text{ nm}^{-1}$ , as a peak of the static structure  
7  
8 factor called “the main peak.” In some liquids, an additional peak, called a “prepeak” is  
9  
10 observed at a wavenumber lower than that of the main peak. The prepeak exhibits the presence  
11  
12 of a characteristic mesoscopic structure whose spatial dimension is much larger than the  
13  
14 intermolecular contact distance. The prepeak structures have been reported on room-temperature  
15  
16 ionic liquids (RTILs)<sup>1,2,3</sup> and higher alcohols,<sup>4,5</sup> and they are ascribed to mesoscopic structures  
17  
18 composed of polar and nonpolar domains.  
19  
20  
21  
22  
23

24  
25 The rheology of structured fluids, including surfactant, colloid, and polymer systems, is  
26  
27 governed by the dynamics of characteristic mesoscopic structures. On the other hand, the shear  
28  
29 viscosity of molecular liquids has been discussed in terms of microscopic liquid structure and  
30  
31 intermolecular interactions. The mechanical properties of molecular and structured fluids have  
32  
33 thus been studied from quite different points of views so far. Although the RTILs and higher  
34  
35 alcohols introduced above belong to molecular liquids, they exhibit a mesoscopic structure that  
36  
37 resembles those seen in surfactant solutions. They can thus bridge the rheology of molecular and  
38  
39 structured fluids. To unveil the character of structured fluids in RTILs and higher alcohols, we  
40  
41 need to evaluate the slow dynamics of the mesoscopic structure and examine its role in  
42  
43 viscoelastic relaxation.  
44  
45  
46  
47  
48

49 In this work, we have chosen a higher alcohol, 3,7-dimethyl-1-octanol, as an example, which  
50  
51 has been a target of studies on the dynamics of supercooled liquids.<sup>6</sup> The branched structure of  
52  
53 the alkyl group prevents crystallization, which enables us to determine the dynamics in a wide  
54  
55 temperature range.  
56  
57  
58  
59  
60

1  
2  
3 The mesoscopic structure of the liquid alcohol appears as a prepeak in a small-angle X-ray  
4 scattering profile.<sup>4,5,7</sup> Its dynamics, described in terms of the intermediate scattering function  
5 (ISF) at the prepeak, is probed by quasielastic scattering spectroscopies. On the other hand, the  
6 dynamics relevant to the shear viscosity is reflected in the viscoelastic relaxation. One of us  
7 (Tsuyoshi Yamaguchi) recently showed computationally that the domain dynamics of higher  
8 alcohols actually contributes to the shear viscosity through the slowest mode of the viscoelastic  
9 relaxation.<sup>7</sup> We shall demonstrate experimentally in this work that a strong relationship between  
10 the domain dynamics and viscoelastic relaxation of higher alcohols exists.  
11  
12

13  
14 The structural dynamics was determined by means of quasielastic scattering spectroscopy  
15 using multiline  $\gamma$ -ray time-domain interferometry.<sup>8,9,10</sup> Utilizing the  $\gamma$ -rays from the  $^{57}\text{Fe}$  nucleus  
16 excited by synchrotron radiation, which shows a relatively narrow energy width of 4.7 neV,  
17 compared with its energy of 14.4 keV, we can measure the slow dynamics of the X-ray ISF in  
18 the ns– $\mu\text{s}$  domain. The quasielastic scattering using  $\gamma$ -ray time-domain interferometry was used  
19 successfully to study the microscopic slow dynamics of glass-forming systems.<sup>11,12</sup> The  
20 technique was also applied to the study of the slow dynamics of the layered structure of smectic-  
21 A liquid crystals.<sup>13</sup> The viscoelastic spectra were determined in a range 5 MHz – 205 MHz and  
22 238 K – 298 K using shear impedance spectroscopy, which has been applied to a variety of  
23 viscous liquids.<sup>14,15,16,17</sup> The details of the experimental methods are described in Supporting  
24 Information.  
25  
26  
27  
28  
29  
30  
31  
32  
33  
34  
35  
36  
37  
38  
39  
40  
41  
42  
43  
44  
45  
46  
47  
48  
49  
50  
51  
52  
53  
54  
55  
56  
57  
58  
59  
60

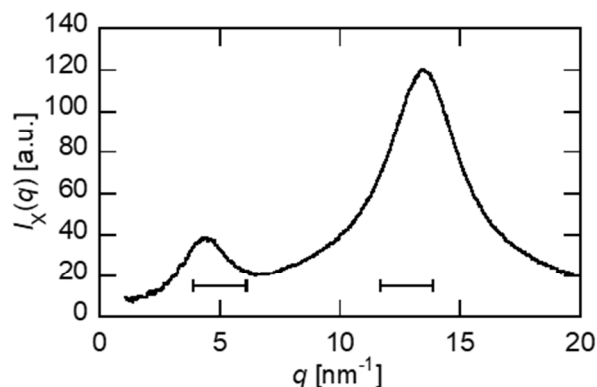


**Figure 1.** The X-ray structure factor of 3,7-dimethyl-1-octanol at room temperature. The two horizontal bars indicate the  $q$ -ranges of the measurement of the ISFs.

The X-ray static structure factor of the sample is shown in Fig. 1. A prepeak is found at the wavenumber  $q = 4.5 \text{ nm}^{-1}$  in addition to the strong main peak at  $q = 13 \text{ nm}^{-1}$ , as in the cases of  $n$ -alcohols.<sup>4,5</sup> The measurements of the quasielastic scattering were performed at two  $q$ -ranges,  $5.0 \pm 1.1 \text{ nm}^{-1}$  and  $12.8 \pm 1.1 \text{ nm}^{-1}$ , covering these two peaks.

The Kohlrausch–Williams–Watts (KWW) functional form,

$$\frac{I(q,t)}{I(q,0)} = f(q) \exp \left[ - \left( \frac{t}{\tau(q)} \right)^{\beta(q)} \right], \quad (1)$$

was applied to the ISFs,  $I(q,t)$ , at both peaks, where  $t$  stands for time, and the parameters  $f$ ,  $\beta$ , and  $\tau$  are related to the amplitude of the slow relaxation mode, the distribution of the relaxation time, and the relaxation time, respectively. The parameters in eq. 1 were optimized to reproduce the time-domain interference signal. The examples of the raw signals and the fitting curves are presented in Fig. S1 of Supporting Information. The values of  $\beta$  were fixed to be 0.60 and 0.66 for the prepeak and the main peak, respectively, as described in Supporting Information, and the

values of  $f$  and  $\tau$  were optimized. The mean relaxation time,  $\langle\tau\rangle$ , was evaluated according to eq. 2,

$$\langle\tau\rangle \equiv \frac{\tau}{\beta} \Gamma\left(\frac{1}{\beta}\right), \quad (2)$$

where  $\Gamma(x)$  stands for the gamma function.

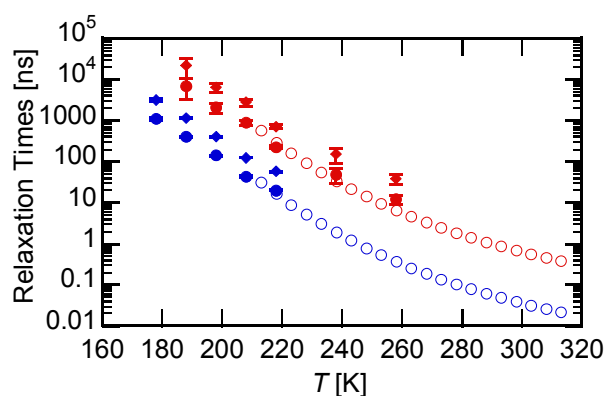
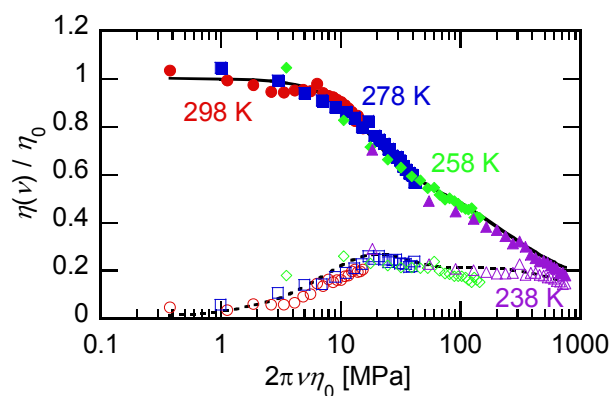


**Figure 2.** The relaxation times of the prepeak (red filled symbols) and main peak (blue filled symbols) are plotted as a function of temperature. The mean relaxation times of the ISF,  $\langle\tau\rangle$  defined by eq. 2, are shown with diamonds, while the mean relaxation times of the squared ISF,  $\langle\tau_2\rangle$  defined by eq. 4, are plotted with circles. They are compared with the relaxation times of the slower (red) and faster (blue) modes of the viscoelastic relaxation,  $\tau_s$  and  $\tau_f$ , respectively, plotted with open circles.

The mean relaxation times of the ISFs at both peaks are exhibited in Fig. 2 with the filled diamonds. We succeeded in determining the relaxation times of ISFs at the prepeak in addition to those at the main peak. The structural relaxation at the prepeak is more than 10 times slower

1  
2  
3 than that at the main peak, and the temperature dependences of the relaxation times at both peaks  
4  
5 are similar to each other.  
6

7  
8 The slower relaxation at the prepeak has been reported in various systems, including RTILs<sup>18,19</sup>  
9  
10 and concentrated electrolyte solutions.<sup>16</sup> In the case of alcohols, Sillrén and coworkers measured  
11  
12 the ISFs of liquid 1-propanol at the prepeak and the main peak, and showed that the relaxation at  
13  
14 the prepeak is several times slower than that at the main peak.<sup>20</sup> Bertrand and coworkers  
15  
16 determined the ISFs of liquid methanol using neutron spin echo (NSE) spectroscopy with isotope  
17  
18 substitution and also demonstrated that the ISF at the prepeak relaxes several times more  
19  
20 slowly.<sup>21</sup> The molecular dynamics (MD) simulation by one of us showed the slower relaxation  
21  
22 at the prepeak in the cases of 1-alcohols, and the separation of the relaxation times at the prepeak  
23  
24 increases with lengthening the alkyl chain.<sup>7</sup> The slow domain dynamics is thus a property of  
25  
26 various liquids with prepeak structures, and 3,7-dimethyl-1-octanol follows the trend.  
27  
28  
29  
30  
31  
32



48 **Figure 3.** The frequency-dependent complex shear viscosity normalized to the steady-state  
49 shear viscosity is plotted against the angular frequency multiplied by the steady-state shear  
50 viscosity. The spectra at four different temperatures are shown with different colors, and the  
51 correspondence between the color and the temperature is given in the panel. The real and  
52  
53  
54  
55  
56  
57  
58  
59  
60

1  
2  
3 imaginary parts of the complex spectra are shown with filled and open symbols, respectively.  
4  
5 The curve fitting using a Cole–Davidson and a Debye function is shown with the solid (real part)  
6  
7 and the dotted (imaginary part) curves, respectively.  
8  
9

10  
11 The frequency-dependent complex shear viscosity,  $\eta(\nu)$ , at four different temperatures is  
12  
13 shown in Fig. S2 of Supporting Information. The spectra normalized to the steady-state shear  
14  
15 viscosity,  $\eta_0$ , are plotted in Fig. 3 against the angular frequency multiplied by  $\eta_0$ . They reduce to  
16  
17 a master curve, which indicates that the temperature dependence of the shear viscosity is  
18  
19 governed by that of the relaxation time.  
20  
21  
22  
23

24 As seen in Fig. 3, the normalized spectra appear to be bimodal, with the reduced relaxation  
25  
26 frequencies of  $2\pi\eta_0\nu \sim 20$  MPa and 400 MPa. The bimodal viscoelastic relaxation of higher  
27  
28 alcohols was suggested by the combination of the transverse and longitudinal ultrasonic  
29  
30 spectroscopies,<sup>22</sup> which was later confirmed by MD simulation.<sup>7</sup> The presence of the bimodal  
31  
32 relaxation has also been confirmed in a deeply supercooled region using conventional  
33  
34 rheometers.<sup>23,24,25</sup>  
35  
36  
37  
38

39 The master curve was approximated by the sum of the Debye and Cole–Davidson functions as  
40  
41

$$\frac{\eta(\nu)}{\eta_0} = \frac{A}{1 + \frac{2\pi i \eta_0 \nu}{G_s}} + \frac{1 - A}{\left(1 + \frac{2\pi i \eta_0 \nu}{G_f}\right)^{\beta_f}}, \quad (3)$$

42  
43  
44  
45  
46  
47  
48 where the first Debye and the second Cole–Davidson terms describe the slower and the faster  
49  
50 relaxation modes, respectively. The relative amplitude of the former is denoted as  $A$ , and  $G_s$  and  
51  
52  $G_f$  are parameters related to the shear moduli of these modes, respectively. The stretch  
53  
54 parameter of the Cole-Davidson function is given by  $\beta_f$ . The fitting curve reproduces the  
55  
56  
57  
58  
59  
60

1  
2  
3 experimental spectra fairly well, as is shown in Fig. 3. Given the values of  $G_s$  and  $G_f$ , the  
4  
5 relaxation times of the slower and faster modes are evaluated from  $\eta_0$  as  $\tau_s = G_s/\eta_0$  and  $\tau_f =$   
6  
7  $G_f/(\beta_f\eta_0)$ , respectively.  
8  
9

10  
11 Mode-coupling theory (MCT) is a theory that can relate the microscopic structural dynamics of  
12  
13 liquids to the macroscopic shear viscosity. It describes the viscoelastic relaxation as a  
14  
15 superposition of the bilinear product of the ISFs.<sup>26</sup> When the dynamics at a particular  
16  
17 wavenumber,  $q^*$  is dominant in a viscoelastic relaxation mode, MCT predicts that the dynamics  
18  
19 of the relaxation mode is proportional to the square of the ISF at  $q^*$ . A comparison between the  
20  
21 viscoelastic relaxation spectra and the squared ISF at a wavenumber thus provides information  
22  
23 on whether the structural dynamics at the wavenumber is related to the shear viscosity. Such a  
24  
25 comparison has been made for various viscous liquids, including RTILs, with the prepeak  
26  
27 structure.<sup>14–16</sup>  
28  
29  
30  
31  
32

33 Provided that the ISF is described by the KWW function, eq. 1, the mean relaxation time of the  
34  
35 squared ISF is given by  
36  
37

$$\langle \tau_2 \rangle \equiv \frac{\tau}{2^{\frac{1}{\beta}} \beta} \Gamma\left(\frac{1}{\beta}\right). \quad (4)$$

38  
39  
40  
41  
42  
43

44 The relaxation times  $\langle \tau_2 \rangle$  at the two peaks are plotted as a function of the reciprocal temperature  
45  
46 in Fig. 2 as the filled circles, and they are compared with the relaxation times of the viscoelastic  
47  
48 spectra,  $\tau_s$  and  $\tau_f$ .  
49  
50

51  
52 As is demonstrated clearly in Fig. 2, the relaxation times  $\langle \tau_2 \rangle$  of the prepeak and the main  
53  
54 peak agree with those of the slower and faster modes of the viscoelastic relaxation, respectively.  
55  
56  
57  
58  
59  
60

1  
2  
3 The correspondence between the structural dynamics and the viscoelastic relaxation has been  
4 suggested by MD simulation.<sup>7</sup> The present experimental results support the prediction of the  
5 MD simulation. In particular, the mesoscopic dynamics of the domain structure of a higher  
6 alcohol is shown to contribute to its shear viscosity through the slower mode of the viscoelastic  
7 relaxation.  
8  
9

10  
11  
12 One may question the difference in the functional forms of the slower mode because the ISF is  
13 approximated by the KWW function with  $\beta = 0.60$ , while the Debye function is used for the  
14 slower mode of the viscoelastic relaxation. Given that the qualities of both ISF and the  
15 viscoelastic spectra is not sufficiently high to analyze the detailed shape of the relaxation spectra,  
16 unfortunately, we limit our discussion simply on the mean relaxation time in this work.  
17  
18  
19  
20  
21  
22  
23  
24  
25  
26  
27

28  
29 Based on the observation of the bimodal shear relaxation of RTILs and the structural  
30 resemblance between RTILs and higher alcohols,<sup>27</sup> Cosby and coworkers proposed that the  
31 slower modes of the shear relaxation of supercooled higher alcohols<sup>23–25</sup> are assigned to the slow  
32 dynamics of the mesoscopic structure.<sup>28</sup> Their assignment on higher alcohols is in harmony with  
33 our present experiment and the previous MD simulation.<sup>7</sup> Sillrén and coworkers compared the  
34 relaxation times of ISFs at the main peak and the prepeak of 1-propanol with the shear relaxation  
35 time estimated from the steady-state shear viscosity and the high-frequency shear modulus in the  
36 supercooled region. They showed that the shear relaxation time corresponds to the relaxation  
37 time of ISF at the main peak rather than to that at the prepeak.<sup>20</sup> Their comparison was however  
38 based on the relaxation time of the ISF itself,  $\langle \tau \rangle$  in this work, and we consider that the  
39 comparison based on the squared ISF will, at least partly, explain the discrepancy between the  
40 prepeak dynamics and the viscoelastic relaxation.  
41  
42  
43  
44  
45  
46  
47  
48  
49  
50  
51  
52  
53  
54  
55  
56  
57  
58  
59  
60

1  
2  
3 Our recent MD simulation demonstrated that the coupling between the shear stress and the  
4 prepeak dynamics exists even in the smallest alcohol, methanol. Yamaguchi and Faraone  
5 studied the coupling between the shear stress and the prepeak structure by means of MD  
6 simulation through the evaluation of the cross-correlation between the shear stress and the  
7 transient two-body density. It has been found that the coupling accompanies the alignment of the  
8 linear hydrogen-bonding chain of methanol along the expansion axis of the shear deformation.<sup>29</sup>  
9  
10  
11  
12  
13  
14  
15  
16  
17

18 The relaxation dynamics of ISF can be probed by various quasielastic scattering experiments  
19 whose time window ranges from fs to  $\mu$ s, which corresponds to the MHz–THz frequency  
20 domain. On the other hand, the viscoelastic relaxation determined by conventional mechanical  
21 rheometers is slower than 10 kHz. The comparison between these two relaxation times thus  
22 requires a large extrapolation of the temperature dependence of the relaxation time, which  
23 inevitably involves a large ambiguity. We thus believe that ultrasonic measurements in the MHz  
24 region are desirable for the determination of viscoelastic properties of liquids for comparison  
25 with structural dynamics obtained by quasielastic scattering spectroscopies.  
26  
27  
28  
29  
30  
31  
32  
33  
34  
35  
36

37 In summary, we determined the structural dynamics of the prepeak of a higher alcohol using  
38 quasielastic  $\gamma$ -ray scattering spectroscopy using time-domain interferometry and found that the  
39 relaxation dynamics of the mesoscopic domain structure agrees with the slower mode of the  
40 viscoelastic relaxation. This indicates that the mesoscopic structure of higher alcohols  
41 contributes to the shear viscosity through the slower mode of the viscoelastic relaxation, as was  
42 suggested by MD simulation. Provided that the mesoscopic structure of higher alcohols is  
43 regarded as a precursor of that of surfactant systems, the shear viscosity of higher alcohols has its  
44 origin common to the structural viscosity of surfactant solutions. Further experimental and  
45  
46  
47  
48  
49  
50  
51  
52  
53  
54  
55  
56  
57  
58  
59  
60

1  
2  
3 theoretical studies will be required for the examination of the applicability of other classes of  
4  
5 liquids such as RTILs.  
6  
7

8  
9 **Supporting Information.** Experimental details, time-domain interference signals, shear  
10  
11 relaxation spectra at various temperatures, and a short review on the relation between the ISF at  
12  
13 the prepeak and the viscoelastic relaxation of RTILs (PDF).  
14  
15

## 16 AUTHOR INFORMATION

### 17 18 19 **ORCID**

20  
21  
22 Tsuyoshi Yamaguchi: 0000-0003-4590-8592  
23  
24

### 25 **Notes**

26  
27  
28 The authors declare no competing financial interests.  
29  
30

### 31 **ACKNOWLEDGMENTS**

32  
33 Tsuyoshi Yamaguchi was supported by the Japan Society for the Promotion of Science (JSPS),  
34  
35 KAKENHI Grant-in-Aid for Scientific Research (C) (No. 16K05514), and Makina Saito was  
36  
37 supported by JSPS KAKENHI Grant-in-Aid for Young Scientists (B) (No. 15K17736). The  
38  
39 construction of the  $\gamma$ -ray quasielastic scattering equipment was partly supported by JSPS  
40  
41 KAKENHI Grant-in-Aid for Scientific Research (S) (No. 24221005). The synchrotron radiation  
42  
43 experiments were performed at the BL09XU of SPring-8 with the approval of the Japan  
44  
45 Synchrotron Radiation Research Institute (JASRI) (Proposal No. 2017A1236).  
46  
47  
48  
49  
50  
51  
52  
53  
54  
55  
56  
57  
58  
59  
60

## REFERENCES

- (1) Lopes, J. N. A. C.; Padua, A. A. H. Nanostructural Organization in Ionic Liquids. *J. Phys. Chem. B* **2006**, *110*, 3330-3335.
- (2) Triolo, A.; Russina, O.; Bleif, H.-J.; di Cola, E. Nanoscale Segregation in Room Temperature Ionic Liquids. *J. Phys. Chem. B* **2007**, *111*, 4641-4644.
- (3) Kashyap, H. K.; Hettige, J. J.; Annapureddy, H. V. R.; Margulis, C. J. SAXS anti-peaks reveal the length-scales of dual positive–negative and polar–apolar ordering in room-temperature ionic liquids. *Chem. Commun.* **2012**, *48*, 5103-5105.
- (4) Tomšič, M.; Bešter-Rogač, M.; Jamnik, A.; Kunz, W.; Touraud, D.; Bergmann, A.; Glatter, O. Nonionic Surfactant Brij 35 in Water and in Various Simple Alcohols: Structural Investigations by Small-Angle X-ray Scattering and Dynamic Light Scattering. *J. Phys. Chem. B* **2004**, *108*, 7021-7032.
- (5) Tomšič, M.; Jamnik, A.; Fritz-Popovski, G.; Glatter, O.; Vlček, L. Structural Properties of Pure Simple Alcohols from Ethanol, Propanol, Butanol, Pentanol, to Hexanol: Comparing Monte Carlo Simulations with Experimental SAXS Data. *J. Phys. Chem. B* **2007**, *111*, 1738-1751.
- (6) Wang, L.-M.; Richert, R. Dynamics of glass-forming liquids. IX. Structural versus dielectric relaxation in monohydroxy alcohols. *J. Chem. Phys.* **2004**, *121*, 11170-11176.
- (7) Yamaguchi, T. Viscoelastic relaxations of high alcohols and alkanes: Effects of heterogeneous structure and translation-orientation coupling. *J. Chem. Phys.* **2017**, *146*, 094511.
- (8) Baron, A. Q. R.; Franz, H.; Meyer, A.; Ruffer, R.; Chumakov, A. I.; Burkel, E.; Petry, W. Quasielastic Scattering of Synchrotron Radiation by Time Domain Interferometry. *Phys. Rev. Lett.* **1997**, *79*, 2823-2826.

1  
2  
3  
4  
5 (9) Saito, M.; Seto, M.; Kitao, S.; Kobayashi, Y.; Kurokuzu, M.; Yoda, Y. Time-domain  
6 interferometry experiments using multi-line nuclear absorbers. *Hyperfine Interact.* **2012**, *206*,  
7 87-90.  
8  
9

10  
11  
12 (10) Saito, M.; Masuda, R.; Yoda, Y.; Seto, M. Synchrotron radiation-based quasi-elastic  
13 scattering using time-domain interferometry with multiline gamma rays. *Sci. Rep.* **2017**, *7*,  
14 12558.  
15  
16  
17

18  
19  
20 (11) Saito, M.; Kitao, S.; Kobayashi, Y.; Kurokuzu, M.; Yoda, Y.; Seto, M. Slow Processes in  
21 Supercooled *o*-Terphenyl: Relaxation and Decoupling. *Phys. Rev. Lett.* **2012**, *109*, 115705.  
22  
23  
24

25  
26 (12) Kanaya, T.; Inoue, R.; Saito, M.; Seto, M.; Yoda, Y. Relaxation transition in glass-  
27 forming polybutadiene as revealed by nuclear resonance X-ray scattering. *J. Chem. Phys.* **2014**,  
28 *140*, 144906.  
29  
30  
31

32  
33 (13) Saito, M.; Seto, M.; Kitao, S.; Kobayashi, Y.; Kurokuzu, M.; Yoda, Y.; Yamamoto, J.  
34 Small and Large Angle Quasi-Elastic Scattering Experiments by Using Nuclear Resonant  
35 Scattering on Typical and Amphiphilic Liquid Crystals. *J. Phys. Soc. Jpn.* **2012**, *81*, 023001.  
36  
37  
38

39  
40 (14) Yamaguchi, T.; Mikawa, K.; Koda, S.; Fujii, K.; Endo, H.; Shibayama, M.; Hamano, H.;  
41 Umebayashi, Y. Relationship between mesoscale dynamics and shear relaxation of ionic liquids  
42 with long alkyl chain. *J. Chem. Phys.* **2012**, *137*, 104511.  
43  
44  
45

46  
47 (15) Yamaguchi, T.; Yonezawa, T.; Koda, S. Study on the temperature-dependent coupling  
48 among viscosity, conductivity and structural relaxation of ionic liquids. *Phys. Chem. Chem.*  
49 *Phys.* **2015**, *17*, 19126-19133.  
50  
51  
52  
53  
54  
55

1  
2  
3  
4  
5 (16) Yamaguchi, T.; Yonezawa, T.; Yoshida, K.; Yamaguchi, T.; Nagao, M.; Faraone, A.;  
6 Seki, S. Relationship between Structural Relaxation, Shear Viscosity, and Ionic Conduction of  
7 LiPF<sub>6</sub>/Propylene Carbonate Solutions. *J. Phys. Chem. B* **2015**, *119*, 15675-15682.  
8  
9

10  
11  
12 (17) Yamaguchi, T. Experimental study on the relationship between the frequency-dependent  
13 shear viscosity and the intermediate scattering function of representative viscous liquids. *J.*  
14 *Chem. Phys.* **2016**, *145*, 194505.  
15  
16  
17

18  
19 (18) Yamamuro, O.; Yamada, T.; Kofu, M.; Nakakoshi, M.; Nagao, M. Hierarchical structure  
20 and dynamics of an ionic liquid 1-octyl-3-methylimidazolium chloride. *J. Chem. Phys.* **2011**,  
21 *135*, 054508.  
22  
23  
24  
25

26  
27 (19) Kofu, M.; Nagao, M.; Ueki, T.; Kitazawa, Y.; Nakamura, Y.; Sawamura, S.; Watanabe,  
28 M.; Yamamuro, O. Heterogeneous Slow Dynamics of Imidazolium-Based Ionic Liquids Studied  
29 by Neutron Spin Echo. *J. Phys. Chem. B* **2013**, *117*, 2773-2781.  
30  
31  
32  
33

34  
35 (20) Sillrén, P.; Matic, A.; Karlsson, M.; Koza, M.; Maccarini, M.; Fouquet, P.; Götz, M.;  
36 Bauer, Th.; Gulich, R.; Lunkenheimer, P.; Loidl, A.; Mattsson, J.; Gainaru, C.; Vynokur, E.;  
37 Schildmann, S.; Bauer, S.; Böhmer, R. Liquid 1-propanol studied by neutron scattering, near-  
38 infrared, and dielectric spectroscopy. *J. Chem. Phys.* **2014**, *140*, 124501.  
39  
40  
41  
42  
43

44  
45 (21) Bertrand, C. E.; Self, J. L.; Copley, J. R. D.; Faraone, A. Nanoscopic length scale  
46 dependence of hydrogen bonded molecular associates' dynamics in methanol. *J. Chem. Phys.*  
47 **2017**, *146*, 194501.  
48  
49  
50  
51  
52

1  
2  
3  
4  
5 (22) Kaatz U.; Behrends, R. High-Frequency Shear Viscosity of Low-Viscosity Liquids. *Int.*  
6  
7 *J. Thermophys.* **2014**, *35*, 2088-2106.  
8  
9

10 (23) Gainaru, C.; Figuli, R.; Hecksher, T.; Jakobsen, B.; Dyre, J. C.; Wilhelm, M.; Böhmer, R.  
11  
12 Shear-Modulus Investigations of Monohydroxy Alcohols: Evidence for a Short-Chain-Polymer  
13  
14 Rheological Response. *Phys. Rev. Lett.* **2014**, *112*, 098301.  
15  
16  
17

18 (24) Gainaru, C.; Wikarek, M.; Pawlus, S.; Paluch, M.; Figuli, R.; Wilhelm, M.; Hecksher, T.;  
19  
20 Jakobsen, B.; Dyre, J. C.; Böhmer, R. Oscillatory shear and high-pressure dielectric study of 5-  
21  
22 methyl-3-heptanol. *Colloid Polym. Sci.* **2014**, *292*, 1913-1921.  
23  
24  
25

26 (25) Hecksher, T. Communication: Linking the dielectric Debye process in mono-alcohols to  
27  
28 density fluctuations. *J. Chem. Phys.* **2016**, *144*, 161103.  
29  
30

31 (26) Yamaguchi, T.; Hirata, F. Site-site mode coupling theory for the shear viscosity of  
32  
33 molecular liquids. *J. Chem. Phys.* **2001**, *115*, 9340-9345.  
34  
35  
36

37 (27) This letter article is focused on the dynamics of a higher alcohol, and we could not share  
38  
39 space to discuss on the dynamics of RTILs in order to improve the readability. Since the  
40  
41 dynamics of RTILs with mesoscopic structure is sometimes related to that of higher alcohols,  
42  
43 however, we summarize the study on the relation between the rheology of RTILs and the ISF at  
44  
45 the prepeak in Sec. S4 of Supporting Information.  
46  
47  
48

49 (28) Cosby, T.; Vicars, Z.; Wang, Y.; Sangoro, J. Dynamic-Mechanical and Dielectric  
50  
51 Evidence of Long-Lived Mesoscale Organization in Ionic Liquids. *J. Phys. Chem. Lett.* **2017**, *8*,  
52  
53 3544-3548.  
54  
55  
56  
57  
58  
59  
60

1  
2  
3  
4  
5 (29) Yamaguchi, T.; Faraone, A. Analysis of shear viscosity and viscoelastic relaxation of  
6 liquid methanol based on molecular dynamics simulation and mode-coupling theory. *J. Chem.*  
7  
8  
9 *Phys.* **2017**, *146*, 244506.  
10  
11  
12  
13  
14  
15  
16  
17  
18  
19  
20  
21  
22  
23  
24  
25  
26  
27  
28  
29  
30  
31  
32  
33  
34  
35  
36  
37  
38  
39  
40  
41  
42  
43  
44  
45  
46  
47  
48  
49  
50  
51  
52  
53  
54  
55  
56  
57  
58  
59  
60